Electrochimica Acta 116 (2014) 111–117

Contents lists available at ScienceDirect

Electrochimica Acta

journal homepage: www.elsevier.com/locate/electacta

In situ assembly of MnO_2 nanowires/graphene oxide nanosheets composite with high specific capacitance

Kai Dai[a], Luhua Lu[b,*], Changhao Liang[c,*], Jianming Dai[c], Qinzhuang Liu[a], Yongxing Zhang[a], Guangping Zhu[a], Zhongliang Liu[a]

[a] College of Physics and Electronic Information, Huaibei Normal University, Huaibei, 235000, PR China
[b] State Key Lab of Advanced Technology for Materials Synthesis and Processing, Wuhan University of Technology, Wuhan 430070, P R China
[c] Key Laboratory of Materials Physics and Anhui Key Laboratory of Nanomaterials and Nanotechnology, Institute of Solid State Physics, Hefei Institutes of Physical Science, Chinese Academy of Sciences, Hefei, 230031, P R China

ARTICLE INFO

Article history:
Received 3 September 2013
Received in revised form 21 October 2013
Accepted 6 November 2013
Available online 20 November 2013

Keywords:
Graphene oxide
MnO_2
Hybrid
Supercapacitors
Electrochemical capacitance

ABSTRACT

Graphene oxide (GO) in situ composited with MnO_2 nanowires was achieved through a hydrothermal process. The morphology and structure of the products were investigated by using field emission scanning electron microscopy, high resolution transmission electron microscopy, X-ray photoelectron spectra and X-ray diffraction. The results showed that the product consisted of α-MnO_2 nanowires with the diameter of 20~40 nm and the length of 0.5~2 μm that well dispersed on the surfaces of GO. The excellent electrochemical performance of as-prepared GO/MnO_2 hybrids was obtained due to the unique chemical interactions between GO and MnO_2. The maximum specific capacitances of 360.3 F/g measured by chronopotentiometry at a current density of 0.5 A/g were obtained in a 1 M Na_2SO_4 aqueous solution. This value is much higher than that of pure MnO_2 nanowire electrodes (128.0 F/g) and commercial MnO_2 microparticles electrodes (22.8 F/g). Furthermore, GO/MnO_2 nanowires hybrids also exhibit good cycling stability with more than 93% capacitance retention over 1000 cycles. The present synthesis strategy may be readily extended to the preparation of other hybrids based on GO nanosheets for potential applications in energy storage and conversion devices.

1. Introduction

Supercapacitor made of metal oxide nanomaterials has attracted an increasing efforts for its high power density, fast energy release and largely improved energy density that is close to battery devices [1–5]. Two type of electrode materials being widely studied for supercapacitor application are nanoscale carbon [6,7], and transition metal oxides materials [8,9]. Carbon nanostructures are of high electrical conductivity favoring the fast energy storage and releasing and the inert structure also supports highly stable electrical double layer capacitance [10,11]. Transition metal oxides are of theoretical super-large pseudocapacitance endowing ultra-high energy density of supercapacitor [12].

Among transition metal oxides, manganese dioxide (MnO_2) has been mostly studied electrode material for supercapacitors thanks to its high theoretical capacity, environmental compatibility, safety, low environmental toxicity, and cost effectiveness [13,14]. However, a large specific volume change commonly occurred in the host matrix of bulk MnO_2 electrode during the cyclic charging/discharging processes, thus leading to pulverization of the electrodes and rapid capacity decay. To minimize the volume change of MnO_2 and increase the electrochemical interface of MnO_2 electrode, one-dimensional (1D) nanostructured MnO_2 has been found to be of good candidate for its low density and good permeation [15–17]. Nevertheless, 1D MnO_2 nanoparticle does not deliver ideal specific capacitance for its poor electrical conductivity and electrochemical dissolution during cycling [18,19]. Thus improving materials' performance substantially to meet the requirements of practical applications is urgently desirable.

To circumvent the obstacles, carbonaceous materials have been chosen as a component for preparing MnO_2-based composites of effectively improved electrical conductivity and electrochemical stability [20]. Compared to other carbon materials such as graphite, active carbon, and carbon nanotubes, graphene is a flat monolayer of carbon atoms with perfect sp^2-hybridized two-dimensional carbon structure [21,22]. The superior electrical conductivity [23], excellent mechanical flexibility[24], high thermal and chemical stability [25], extremely high specific surface area (2630 m^2/g) and easy functionalization make graphene good substrate to produce graphene-based functional composites [26,27]. Moreover, GO has abundant active polar functional groups making it of similar performance with that of surfactants [28–30]. For example,

* Corresponding author.
E-mail addresses: lhlu@whut.edu.cn (L. Lu), chliang@issp.ac.cn (C. Liang).

0013-4686/$ – see front matter © 2013 Elsevier Ltd. All rights reserved.
http://dx.doi.org/10.1016/j.electacta.2013.11.036

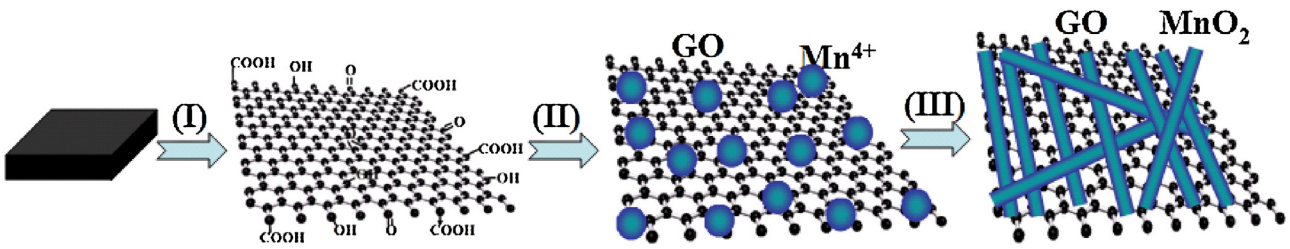

Fig. 1. Illustration of three steps for GO/MnO_2 hybrid formation. (I) exfoliation of graphite oxide into GO sheets, (II) formation of MnO_2 nuclei and interaction between GO sheets and MnO_2 through hydrogen bonding, (III) hydrothermal treatment at 160 °C for 24 h to produce GO/MnO_2 hybrid materials.

Wu et al. reported a high-voltage asymmetric electrochemical capacitor based on graphene as negative electrode and MnO_2 nanowire/graphene composite as positive electrode in a neutral aqueous Na_2SO_4 solution with high energy density [31]. Peng et al. obtained hybrid nanostructures of quasi-2D ultrathin MnO_2/graphene nanosheets for high-performance in-plane supercapacitor [32]. Mao et al. prepared nanostructured MnO_2 with different morphologies (amorphous, lamellar and needle-like) is incorporated with tetrabutylammonium hydroxide stabilized graphene with different mass ratios and investigated their electrochemical properties [33]. However, the achievement of this composite structure requires complex and accurate control of the experimental condition, which is unfavorable for their large scale usage. And the performance of reported materials needs to be further improved.

Here, we report the fabrication of highly uniform GO/MnO_2 nanowire composite on a gram-scale in an aqueous solution without any catalysts or templates untilized. The electrochemical properties of as-obtained nanocomposites electrode were investigated together with electrodes from pure MnO_2 nanowires and commercial bulk MnO_2 particles for comparison. The electrochemical specific capacitance of GO/MnO_2 composite electrode is as high as 360.3 F/g. Cyclic stability test shows that 93% preservation could be preserved after 1000 time cycles.

2. Material and methods

2.1. Materials

Natural graphite powder (325 mesh) and polyvinylidene difluoride (PVDF) was commercially obtained from Alfa-Aesar. Hydrochloric acid (37%, HCl), concentrated sulfuric acid (98%, H_2SO_4), and potassium permanganate ($KMnO_4$) were purchased from Shanghai Chemical Reagent Co., Ltd (China). Sodium nitrate ($NaNO_3$), sodium sulfate (Na_2SO_4), potassium persulfate ($K_2S_2O_8$), phosphorus pentoxide (P_2O_5) hydrogen peroxide (30%, H_2O_2), and manganese sulfate ($MnSO_4$) were purchased from Sinopharm Chemical Reagent Corp (China). All reactants were used as received without further purification. Double distilled water was used during the experimental process. The experiments were carried out at room temperature and humidity.

2.2. Preparation of GO

GO was synthesized by the modified Hummers' method [34,35]. In detail, 3 g of graphite was put into a mixture of 12 mL of concentrated H_2SO_4, 2.5 g of $K_2S_2O_8$, and 2.5 g of P_2O_5. The solution was heated to 80 °C and kept stirring for 4.5 h in oil bath. Then the mixture was diluted with 500 mL of water, and the product was obtained by filtering using 0.2μm Nylon film and dried under ambient condition. Thereafter, 15 g $KMnO_4$ was added gradually with stirring, to prevent the temperature of the mixture from exceeding 10 °C. The ice bath was then removed and the mixture was stirred at 35 °C for 2 h. The reaction was terminated by adding 700 mL of water and 20 mL of 30% H_2O_2 solution. Finally, the GO was recovered by filtration and drying.

2.3. Synthesis of GO/MnO_2 nanowires

1.736 g $MnSO_4$, 3.936 g $KMnO_4$ and 0.040 g GO were initially dissolved in 100 mL water and vigorously stirred for 1 h. And then, the mixture was further transferred into a 50 mL Teflon-lined autoclave and subsequently heated at 160 °C for 24 h. When it cooled down to room temperature naturally, the products were harvested by centrifugation and washed with water, and were finally dried at 80 °C for 4 h.

2.4. Material characterization

The crystal structure of the products was characterized by X-ray diffraction (XRD) using a DX-2000 X-ray powder diffractometer. The morphology and structure of the synthesized materials were investigated by using S4800 field emission scanning electron microscopy (FESEM) attached with Inca Energy-dispersive X-ray spectroscopy (EDX) and a Tecnai G2 F20 S-Twin High resolution transmission electron microscopy (HRTEM). The Brunauer-Emmett-Teller (BET) specific surface area values were performed using ASAP2020 instrument. The electronic valence states of nanocomposite were analyzed by X-ray photoelectron spectra (XPS) using a Thermo ESCALAB 250 with Al $K\alpha$ line at 150 W.

2.5. Electrochemical Measurement

The working electrodes of electrochemical capacitors were formed by mixing the synthesized powder with 15 wt.% graphite and 5 wt.% PVDF binder of the total electrode mass. The mixtures were pressed onto nickel foam current collectors with an area of 10×10 mm^2 to form electrodes. The electrochemical measurements were done in a three-electrode experimental setup on a CHI 660D electrochemical workstation using 1 M Na_2SO_4 aqueous as electrolyte. Pt foil and a saturated calomel electrode (SCE) were used as the counter and reference electrodes, respectively. The specific capacitance C_S (F/g), of the electrode material was calculated from the discharge curve according to the following equation [36,37]:

$$C_S = I\Delta t/(\Delta Vm) \quad (1)$$

Where: I is the discharge current (A), $\triangle t$ is the discharge time (s), $\triangle V$ is the voltage change (V) excluding IR drop in the discharge process, and m is the mass of the electrode material (g) excluding the binder and conductive graphite.

3. Results and Discussion

Fig. 1 present the designed formation processes for obtaining GO/MnO_2 nanowires hybrids. GO sheets have their basal planes

decorated mostly with epoxy and hydroxyl groups, while carbonyl and carboxyl groups are located at the edges by the modified Hummers' method [38]. These functional groups, acting as anchor sites, enable the subsequent in situ formation of nanostructures attaching on the surfaces and edges of GO sheets. The structural framework of MnO_2 is made of basic MnO_6 octahedron units, which are linked in different ways to produce MnO_2 crystals with different crystallographic forms and morphologies. At the initial stage, Mn^{2+} ions, formed by the dissolution of $MnSO_4$, favorably bind with the O atoms of the negatively charged oxygen-containing functional groups on GO sheets via an electrostatic force [39]. With the addition of a solution of $KMnO_4$ at a relatively higher temperature, a large number of Mn^{4+} ions nuclei were formed in a short time from the redox reaction occurring between Mn^{2+} and Mn^{7+}. The chemical reaction involved in the growth of α-MnO_2 is according to the equation (2):

$$3MnSO_4 + 2KMnO_4 + 2H_2O \rightarrow 5MnO_2 + 2H_2SO_4 + K_2SO_4 \quad (2)$$

The MnO_2 molecules may form bonds with O atoms of the functional groups via an intermolecular hydrogen bond or a covalent coordination bond, acting as anchor sites for the crystals growth.

Fig. 2 shows the XRD pattern of GO, MnO_2 nanowires and GO/MnO_2 nanowires hybrid. A clear XRD peak of GO is centered at 2θ= 9.66°, which is corresponding to the (001) reflection of stacked GO sheets, suggesting the introduction of oxygen-containing groups on GO sheets [40]. In the XRD pattern of GO/MnO_2, all the peaks of GO/MnO_2 hybrid and MnO_2 were distinguishable. The diffraction angles at 2θ=12.98°, 18.24°, 25.72°, 28.86°, 37.66°, 41.90°, 49.80°, 56.28°, 60.32°, 65.60° and 69.24°, can be assigned to (100), (200), (220), (310), (211), (301), (411), (600), (521), (002) and (541) crystal planes of a pure tetragonal the α-MnO_2 phase (JCPDS, card no: 44-0141, a = 9.7845 Å, c = 2.8630 Å),

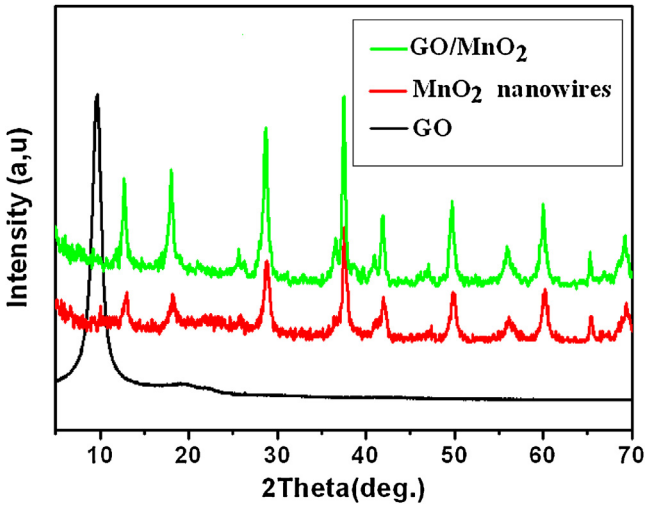

Fig. 2. XRD patterns of GO, MnO_2 nanowires and GO/MnO_2 composite.

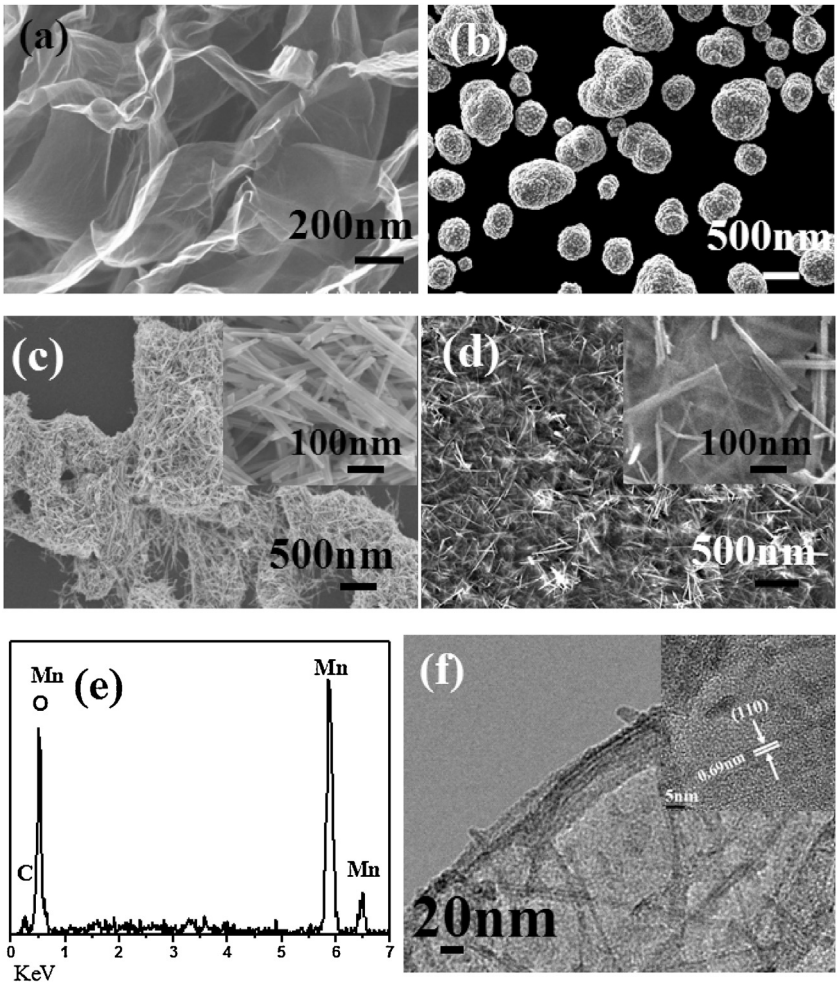

Fig. 3. SEM images of (a) GO, (b) commercial MnO_2 microparticles, (c) MnO_2 nanowires and (d) GO/MnO_2 nanowires hybrid, EDX spectrum (e) of GO/MnO_2 hybrid, and HRTEM image of (f) GO/MnO_2 hybrid.

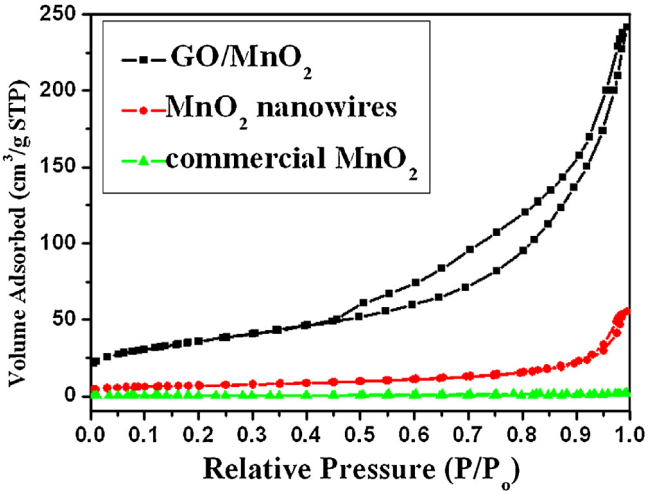

Fig. 4. The nitrogen adsorption-desorption isotherms of GO/MnO_2, MnO_2 nanowires and commercial MnO_2 particles.

respectively. The XRD peak positions and shapes of GO/MnO_2 are similar with those of MnO_2, no obvious diffraction peaks of GO were observed. Previous studies have shown that the diffraction peaks become weakened or even disappear whenever the regular stacks of GO are separated by inorganic units [41,42].

Fig. 3 presents typical SEM and TEM images of the as-synthesized α-MnO_2 nanowires and GO/α-MnO_2 hybrid electrode materials. As indicated in Fig. 3b and 3c, the size of commercial α-MnO_2 is about 0.5~2μm, the α-MnO_2 nanowires thereby synthesized had a diameter of 20~40 nm and a length of 0.5~2μm, which were all well separated without adhering to each other. The SEM image in Fig. 3d presents well-dispersed α-MnO_2 nanowires on the surface of GO without excessive wrapping by the GO sheets. The surface attachment of α-MnO_2 nanowires, instead of complete or partial wrapping by GO, assured full exposure of both GO sheets and α-MnO_2 nanowires to Na^+ and H^+ ions during charge/discharge cycles. Combining the two materials as electrode material may offer significant synergistic effects arising from the high electrical conductivity and large surface area of GO sheets and potentially excellent catalytic performance of α-MnO_2 nanowires. The HRTEM image in Fig. 3f reveals clear lattice fringes of well-crystallized α-MnO_2 nanowire. The distance between the two fringes was 0.69 nm, corresponding to the (110) lattice planes [43].

Fig. 4 shows the nitrogen adsorption–desorption isotherms for GO, MnO_2 nanowires and GO/MnO_2 nanowires hybrids. GO/MnO_2 nanowires hybrids show a distinct hysteresis in the larger range from 0.45 to 1.0 P/P_0 in Fig. 3a, indicating the presence of mesopores possibly formed by the porous stacking of component nanoparticles [44]. The BET surface area of GO/MnO_2 nanowires hybrid (128.3 m^2/g) is much larger than that of MnO_2 nanowires (23.7 m^2/g), and commercial MnO_2 microparticles (0.8 m^2/g), which may allow an efficient contact of GO/MnO_2 with the electrolyte.

XPS spectra of C1s, O1s and Mn2p orbitals of the GO/MnO_2 hybrid are shown in Fig. 5. Fig. 5a shows the high-resolution spectra of C1s, which can be fitted as three peaks at binding energies of 284.80, 286.32 and 288.38 eV, implying three different chemical environments of carbon existing in the sample. The peaks at 284.80 eV can be assigned to contributions of C-C (sp^2) bonds [45]. While the peak at 286.32 eV is due to the existence of C-OH bonds and the peak at 288.38 eV comes from the existence of C-OOH bonds [46,47]. As indicated in Fig. 5b, the binding energies of Mn 2p3/2 and Mp1/2 are centered at 642.26 and 653.90 eV, respectively, in well agreement with those of pure α-MnO_2. Fig. 5c shows the high-resolution spectra of O1s. In the case of GO/MnO_2 hybrid, the curve

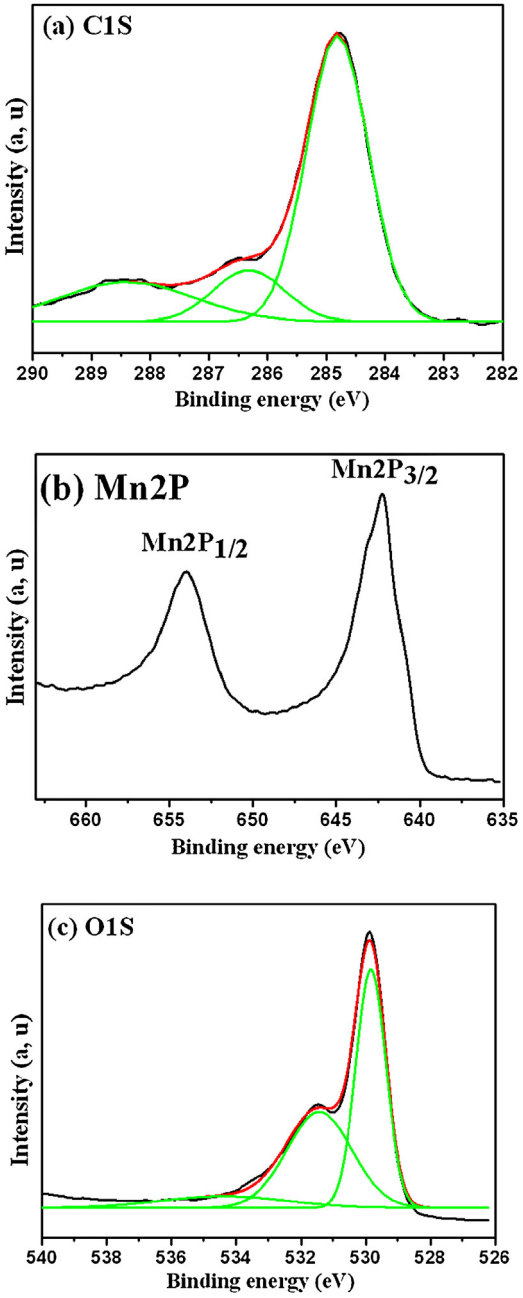

Fig. 5. XPS spectra measured at the surface of GO/MnO_2.

fitting of O 1s peak basically indicates three components centered at 529.84, 531.50 and 534.22 eV. The O1s peak at 529.84 eV is assigned to the oxygen bonded with manganese (Mn-O) in α-MnO_2 crystal lattice [48]. The latter two peaks are commonly ascribed to the surface oxygen complexes of carbon phase [49,50]. Clearly, all the manganese cations in the hybrid material are in the oxidized states. On the basis of the quantitative analysis of XPS data, the atomic percentages of C, O and Mn are estimated to be 32.6, 45.7, and 21.7%, respectively.

Fig. 6a 6b and 6c show the charge-discharge curves of the synthesized GO/MnO_2, α-MnO_2 nanowires and commercial α-MnO_2 particles at varied current densities (0.5–5 A/g) within a voltage range of 0.0 and 1.0 V. According to equation (1), the specific capacitance of three samples calculated at 0.5, 1, 3 and 5 A/g is shown in fig. 6d. The specific capacitance reaches 360.3 F/g at a current density of 0.5 A/g and remains at 223.6 F/g even at 5.0 A/g in

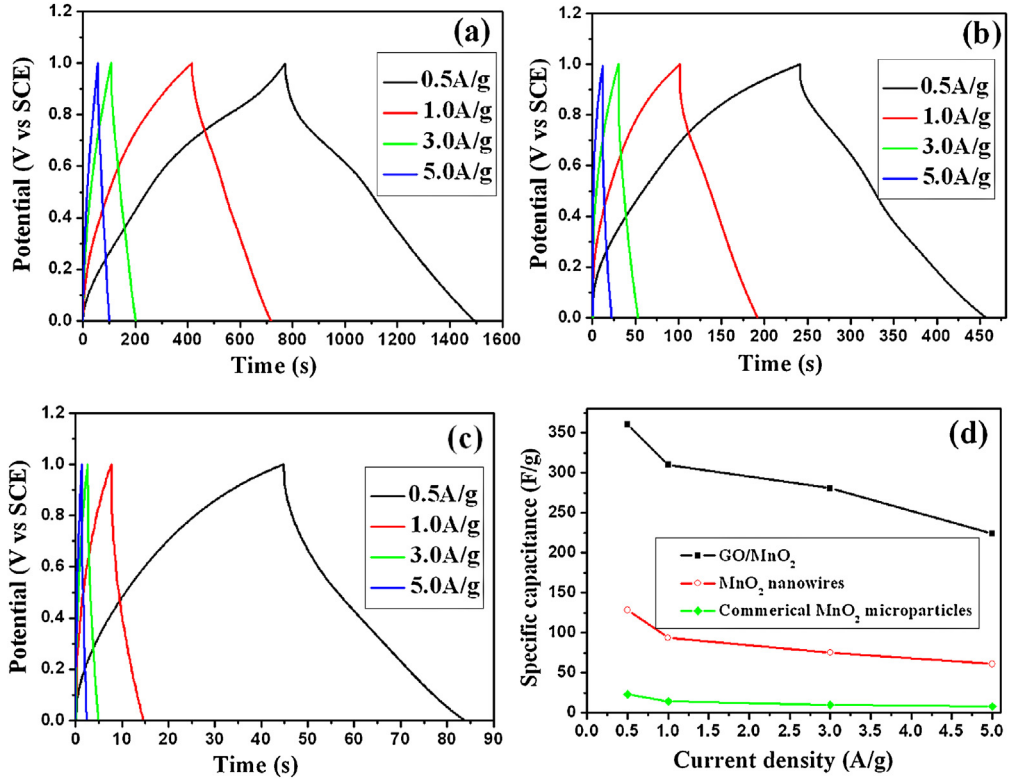

Fig. 6. Galvanostatic charge-discharge of (a) GO/MnO_2, (b) MnO_2 nanowires and (c) commercial MnO_2 particle electrodes at current density of 0.5, 1.0, 3.0 and 5.0 A/g, and (d) the specific capacitances calculated by different current densities of GO/MnO_2, MnO_2 nanowires and commercial MnO_2 particles.

1 M Na_2SO_4 aqueous solution, which was almost triple of that of pure MnO_2 nanowire (128.0 F/g) electrodes and 16 times of that of commercial MnO_2 microparticle (22.8 F/g) electrodes. The unique GO/MnO_2 hybrids not only exhibit high capacitance but also high stable electrochemical performance at high current densities.

Fig. 7a presents the cyclic voltammetry (CV) curves of GO/MnO_2, α-MnO_2 nanowire and commercial α-MnO_2 particle electrodes within the electrochemical window from -0.2 to 0.8 V under the scan rate of 5 mV/s. GO/MnO_2 electrodes yielded the largest current and resulted in much higher capacitance, which is believed to be due to the synergistic effects from GO and MnO_2 nanowire of composite electrodes that further boosts the electrical conductivity and contributes the redox-based pseudocapacitance. CV curves of GO/MnO_2 nanowires at different potential scan rates ranging from 5 to 100 mV/s are shown in Fig. 7b. At 5 mV/s, GO/MnO_2 show almost ideal capacitive behavior. Due to the internal resistance of MnO_2 nanowire electrode, the curve is gradually distorted from rectangular shape as the scan rate increases. The large CV loops result from the superposition of electric double-layer capacitance and pseudocapacitance rising from the reaction between electrode and the H^+ or Na^+ ion from the electrolyte [51], and the electrochemical reaction can be expressed as follows [52]:

$$MnO_2 + C^+ + e^- \leftrightarrow MnOOC(C^+ = Na^+, H^+) \quad (3)$$

At a low current density, the diffusion of ions from the electrolyte can gain access to almost all available area of the electrode, leading to a complete insertion reaction, and therefore a higher capacitance. When the scan rate increases, the effective interaction between the ion and the electrode is greatly reduced, there is a reduction in capacitance.

Fig. 8 shows the cyclic electrochemical performance of the GO/MnO_2 nanowires electrode by galvanostatic charging-discharging at a current density of 0.5 A/g within a voltage range of 0.0 and 1.0 V for 1000 cycles, which reveals that cycling does

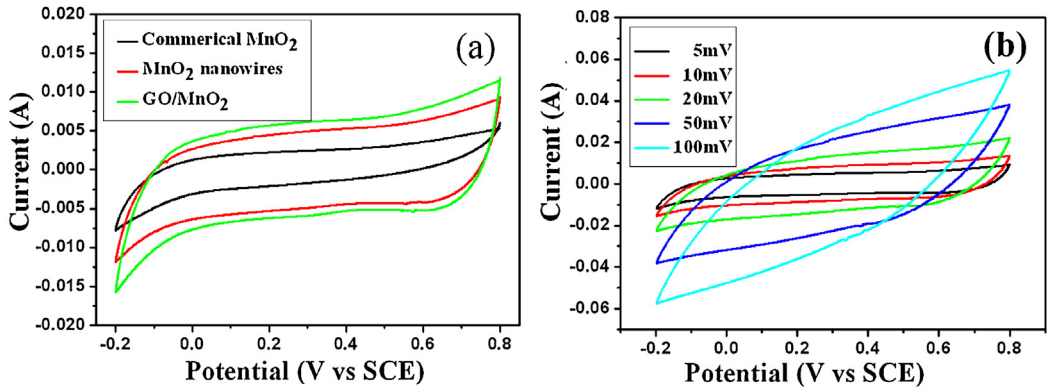

Fig. 7. CV curves of (a) GO/MnO_2, MnO_2 nanowires and commercial MnO_2 particles at 5 mV/s, and (b) GO/MnO_2 nanowires hybrids at different scan rate.

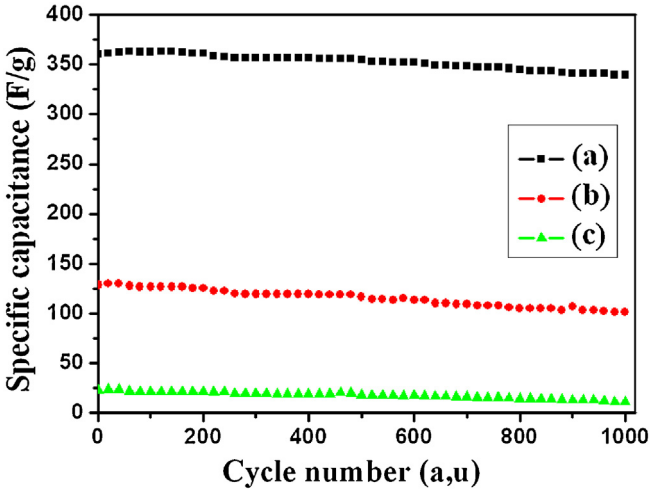

Fig. 8. Cycle performance of (a) GO/MnO_2, (b) MnO_2 nanowires and (c) commercial MnO_2 particles measured at current density of 0.5 A/g.

not cause noticeable degradation of the nanostructure electrode. More than 93% of the initial capacitance was preserved after 1000 charge-dischange cycles. The unique nanosheet-nanowire structure of GO/MnO_2 nanowires composite effectively prevents the aggregation of GO and MnO_2 nanowires and consequently provides high specific surface area, which is favorable for fast hydrated ion transport in the electrolyte to the surfaces of both GO and MnO_2 nanowires. Furthermore, the superior electrical conductivity of GO can significantly decrease the internal resistance of electrode by the construction of a conductive network. MnO_2 nanowires with small diameters is also helpful for shortening ion diffusion path, which can greatly reduce the charge transfer resistance and ionic diffusion resistance [53]. This kind of relatively low-cost GO/MnO_2 composite combines high capacitance and long cycling life in green neutral aqueous electrolytes rather than acetonitrile or alkali-based solvents. Therefore, the present GO/MnO_2 nanowires could be of an attractive candidate material for supercapacitor electrodes.

4. Conclusions

In summary, a novel route for easy and scale synthesis of GO/MnO_2 nanowires hybrid was developed based on a controllable chemical approach. The electrode made from GO/MnO_2 composite exhibited good capacitive performance as high as 360.3 F/g at 0.5 A/g. Moreover, more than 93% of the original capacitance of GO/MnO_2 could be preserved after 1000 cycles of charge-discharge. This simple and green material preparation technique may be extended to the synthesis of other GO based nanocomposteshybrids, and the GO/MnO_2 nanowires hybrid here expected to be used for potential electrode materials for practical supercapacitors.

Acknowledgements

This work was supported by the National Natural Science Foundation of China (51302101, 21303129 and 11174287), the key Foundation of Educational Commission of Anhui Province (KJ2012A250) and the Huaibei Science and Technology Development Funds (20110305).

References

[1] Z. Yang, J. Zhang, M.C. Kintner-Meyer, X. Lu, D. Choi, J.P. Lemmon, J. Liu, Electrochemical energy storage for green grid, Chem. Rev. 111 (2011) 3577.
[2] M. Zhi, C. Xiang, J. Li, M. Li, N. Wu, Nanostructured carbon-metal oxide composite electrodes for supercapacitors: a review, Nanoscale 5 (2012) 72.
[3] B. Xu, S. Yue, Z. Sui, X. Zhang, S. Hou, G. Cao, Y. Yang, What is the choice for supercapacitors: graphene or graphene oxide? Energ. Environ. Sci. 4 (2011) 2826.
[4] Y.L. Chen, Z.A. Hu, Y.Q. Chang, H.W. Wang, Z.Y. Zhang, Y.Y. Yang, H.Y. Wu, Zinc Oxide/Reduced Graphene Oxide Composites and Electrochemical Capacitance Enhanced by Homogeneous Incorporation of Reduced Graphene Oxide Sheets in Zinc Oxide Matrix, J. Phys. Chem. C 115 (2011) 2563.
[5] H. Zhang, G. Cao, Y. Yang, Carbon nanotube arrays and their composites for electrochemical capacitors and lithium-ion batteries, Energ. Environ. Sci. 2 (2009) 932.
[6] V. Barranco, M.A. Lillo-Rodenas, A. Linares-Solano, A. Oya, F. Pico, J. Ibañez, F. Agullo-Rueda, J.M. Amarilla, J.M. Rojo, Amorphous Carbon Nanofibers and Their Activated Carbon Nanofibers as Supercapacitor Electrodes, J. Phys. Chem. C 114 (2010) 10302.
[7] H. Jiang, P.S. Lee, C. Li, 3D carbon based nanostructures for advanced supercapacitors, Energ. Environ. Sci. 6 (2013) 41.
[8] J.H. Zhong, A.L. Wang, G.R. Li, J.W. Wang, Y.N. Ou, Y.X. Tong, Co_3O_4/$Ni(OH)_2$ composite mesoporous nanosheet networks as a promising electrode for supercapacitor applications, J. Mater. Chem. 22 (2012) 5656.
[9] Z. Lu, Z. Chang, W. Zhu, X. Sun, Beta-phased $Ni(OH)_2$ nanowall film with reversible capacitance higher than theoretical Faradic capacitance, Chem. Commun. 47 (2011) 9651.
[10] X. Huang, X. Qi, F. Boey, H. Zhang, Graphene-based composites, Chem. Soc. Rev. 41 (2012) 666.
[11] Y. Wang, Z. Shi, Y. Huang, Y. Ma, C. Wang, M. Chen, Y. Chen, Supercapacitor Devices Based on Graphene Materials, J. Phys. Chem. C 113 (2009) 13103.
[12] P. Simon, Y. Gogotsi, Materials for electrochemical capacitors, Nat. Mater. 7 (2008) 845.
[13] Q. Li, Z.L. Wang, G.R. Li, R. Guo, L.X. Ding, Y.X. Tong, Design and synthesis of MnO_2/Mn/MnO_2 sandwich-structured nanotube arrays with high supercapacitive performance for electrochemical energy storage, Nano Lett. 12 (2012) 3803.
[14] V. Subramanian, H. Zhu, R. Vajtai, P.M. Ajayan, B. Wei, Hydrothermal Synthesis and Pseudocapacitance Properties of MnO_2 Nanostructures, J. Phys. Chem. B 109 (2005) 20207.
[15] L. Yuan, X.H. Lu, X. Xiao, T. Zhai, J. Dai, F. Zhang, B. Hu, X. Wang, L. Gong, J. Chen, C. Hu, Y. Tong, J. Zhou, Z.L. Wang, Synthesis of Single-Crystal Tetragonal α-MnO_2 Nanotubes, ACS Nano 6 (2012) 656.
[16] S. Chen, J. Zhu, Q. Han, Z. Zheng, Y. Yang, X. Wang, Shape-Controlled Synthesis of One-Dimensional MnO_2 via a Facile Quick-Precipitation Procedure and its Electrochemical Properties, Cryst. Growth Des. 9 (2009) 4356.
[17] J. Luo, H.T. Zhu, H.M. Fan, J.K. Liang, H.L. Shi, G.H. Rao, J.B. Li, Z.M. Du, Z.X. Shen, Synthesis of Single-Crystal Tetragonal α-MnO_2 Nanotubes, J. Phys. Chem. C 112 (2008) 12594.
[18] W. Wei, X. Cui, W. Chen, D.G. Ivey, Manganese oxide-based materials as electrochemical supercapacitor electrodes, Chem. Soc. Rev. 40 (2011) 1697.
[19] J. Zhang, C.M. Li, Nanoporous metals: fabrication strategies and advanced electrochemical applications in catalysis, sensing and energy systems, Chem. Soc. Rev. 41 (2012) 7016.
[20] S. Nardecchia, D. Carriazo, M.L. Ferrer, M.C. Gutiérrez, F. del Monte, Three dimensional macroporous architectures and aerogels built of carbon nanotubes and/or graphene: synthesis and applications, Chem. Soc. Rev. 42 (2013) 794.
[21] Y.W. Son, M.L. Cohen, S.G. Louie, Energy Gaps in Graphene Nanoribbons Phys, Rev. Lett. 97 (2006) 216803.
[22] J.C. Meyer, A.K. Geim, M.I. Katsnelson, K.S. Novoselov, T.J. Booth, S. Roth, The structure of suspended graphene sheets, Nature 446 (2007) 60.
[23] S. Park, R.S. Ruoff, Chemical methods for the production of graphenes, Nat. Nanotechnol. 4 (2009) 217.
[24] B.Z. Jang, C. Liu, D. Neff, Z. Yu, M.C. Wang, W. Xiong, A. Zhamu, Graphene surface-enabled lithium ion-exchanging cells: next-generation high-power energy storage devices, Nano Lett. 11 (2011) 3785.
[25] S.H. Aboutalebi, A.T. Chidembo, M. Salari, K. Konstantinov, D. Wexler, H.K. Liu, S.X. Dou, Comparison of GO, GO/MWCNTs composite and MWCNTs as potential electrode materials for supercapacitors, Energ. Environ. Sci. 4 (2011) 1855.
[26] M.D. Stoller, S. Park, Y. Zhu, J. An, R.S. Ruoff, Graphene-based ultracapacitors, Nano Lett. 8 (2008) 3498.
[27] D. Li, M.B. Muller, S. Gilje, R.B. Kaner, G.G. Wallace, Processable aqueous dispersions of graphene nanosheets, Nat. Nanotechnol. 3 (2008) 101.
[28] R.B. Rakhi, W. Chen, D. Cha, H.N. Alshareef, High performance supercapacitors using metal oxide anchored graphene nanosheet electrodes, J. Mater. Chem. 21 (2011) 16197.
[29] N. Soin, S.S. Roy, S.K. Mitra, T. Thundat, J.A. McLaughlin, Nanocrystalline ruthenium oxide dispersed Few Layered Graphene (FLG) nanoflakes as supercapacitor electrodes, J. Mater. Chem. 22 (2012) 14944.
[30] G. Yu, L. Hu, N. Liu, H. Wang, M. Vosgueritchian, Y. Yang, Y. Cui, Z. Bao, Enhancing the supercapacitor performance of graphene/MnO_2 nanostructured electrodes by conductive wrapping, Nano Lett. 11 (2011) 4438.
[31] Z.S. Wu, W. Ren, D.W. Wang, F. Li, B. Liu, H.M. Cheng, High-Energy MnO_2 Nanowire/Graphene and Graphene Asymmetric Electrochemical Capacitors, ACS Nano 4 (2010) 5835.
[32] L. Peng, X. Peng, B. Liu, C. Wu, Y. Xie, G. Yu, Ultrathin Two-Dimensional MnO_2/Graphene Hybrid Nanostructures for High-Performance, Flexible Planar Supercapacitors, Nano Lett. 13 (2013) 2151.
[33] L. Mao, K. Zhang, H.S.O. Chan, J. Wu, Nanostructured MnO_2/graphene composites for supercapacitor electrodes: the effect of morphology, crystallinity and composition, J. Mater. Chem. 22 (2012) 1845.

[34] W.S. Hummers, R.E. Offeman, Preparation of Graphitic Oxide, J. Am. Chem. Soc. 80 (1958) 1339.
[35] Y. Wang, Y.M. Li, L.H. Tang, J. Lu, J.H. Li, Application of Graphene Modified Electrode for Selective Detection of Dopamine, Electrochem. Commun. 11 (2009) 889.
[36] B. Gao, C. Yuan, L. Su, L. Chen, X. Zhang, Nickel oxide coated on ultrasonically pretreated carbon nanotubes for supercapacitor, J Solid State Electr. 13 (2008) 1251.
[37] C. Guan, X. Li, Z. Wang, X. Cao, C. Soci, H. Zhang, H.J. Fan, Nanoporous walls on macroporous foam: rational design of electrodes to push areal pseudocapacitance, Adv. Mater. 24 (2012) 4186.
[38] Y. Xu, G. Shi, Assembly of chemically modified graphene: methods and applications, J. Mater. Chem. 21 (2011) 3311.
[39] Z. Lei, F. Shi, L. Lu, Incorporation of MnO_2-coated carbon nanotubes between graphene sheets as supercapacitor electrode, ACS Appl. Mater. Interf. 4 (2012) 1058.
[40] C. Xu, X. Wang, Fabrication of Flexible Metal-Nanoparticle Films Using Graphene Oxide Sheets as Substrates, Small 5 (2009) 2212.
[41] L. Qiu, X. Yang, X. Gou, W. Yang, Z.F. Ma, G.G. Wallace, D. Li, Dispersing Carbon Nanotubes with Graphene Oxide in Water and Synergistic Effects between Graphene Derivatives, Chem.-Eur. J. 16 (2010) 10653.
[42] R. Pasricha, S. Gupta, A.K. Srivastava, A. Facile, Novel Synthesis of Ag–Graphene-Based nanocomposites, Small 5 (2009) 2253.
[43] J. Zhu, W. Shi, N. Xiao, X. Rui, H. Tan, X. Lu, H.H. Hng, J. Ma, Q. Yan, Oxidation-etching preparation of MnO_2 tubular nanostructures for high-performance supercapacitors, ACS Appl. Mater. Interf. 4 (2012) 2769.
[44] J.Y. Baek, H.W. Ha, I.Y. Kim, S.J. Hwang, Hierarchically Assembled 2D Nanoplates and 0D Nanoparticles of Lithium-Rich Layered Lithium Manganates Applicable to Lithium Ion Batteries, J. Phys. Chem. C 113 (2009) 17392.
[45] R. Bhowmick, S. Rajasekaran, D. Friebel, C. Beasley, L. Jiao, H. Ogasawara, H. Dai, B. Clemens, A. Nilsson, Hydrogen Spillover in Pt-Single-Walled Carbon Nanotube Composites: Formation of Stable C - H Bonds, J. Am. Chem. Soc. 133 (2011) 5580.
[46] Q. Xiang, J. Yu, M. Jaroniec, Enhanced photocatalytic H-production activity of graphene-modified titania nanosheets, Nanoscale 3 (2011) 3670.
[47] T.I.T. Okpalugo, P. Papakonstantinou, H. Murphy, J. McLaughlin, N.M.D. Brown, High resolution XPS characterization of chemical functionalized MWCNTs and SWCNTs, Carbon 43 (2005) 153.
[48] Q.T. Qu, P. Zhang, B. Wang, Y.H. Chen, S. Tian, Y.P. Wu, R. Holze, Electrochemical Performance of MnO_2 Nanorods in Neutral Aqueous Electrolytes as a Cathode for Asymmetric Supercapacitors, J. Phys. Chem. C 113 (2009) 14020.
[49] Q.J. Xiang, J.G. Yu, M. Jaroniec, Preparation and Enhanced Visible-Light Photocatalytic H_2-Production Activity of Graphene/C_3N_4 Composites, J. Phys. Chem. C 115 (2011) 7355.
[50] O. Akhavan, E. Ghaderi, Photocatalytic Reduction of Graphene Oxide Nanosheets on TiO_2 Thin Film for Photoinactivation of Bacteria in Solar Light Irradiation, J. Phys. Chem. C 113 (2009) 20214.
[51] G. Yu, L. Hu, M. Vosgueritchian, H. Wang, X. Xie, J.R. McDonough, X. Cui, Y. Cui, Z. Bao, Solution-processed graphene/MnO_2 nanostructured textiles for high-performance electrochemical capacitors, Nano Lett. 11 (2011) 2905.
[52] B.G. Choi, Y.S. Huh, W.H. Hong, H.J. Kim, H.S. Park, Electrochemical assembly of MnO_2 on ionic liquid-graphene films into a hierarchical structure for high rate capability and long cycle stability of pseudocapacitors, Nanoscale 4 (2012) 5394.
[53] C.L. Xu, Y.Q. Zhao, G.W. Yang, F.S. Li, H.L. Li, Mesoporous Nanowire Array Architecture of Manganese Dioxide for Electrochemical Capacitor Applications, Chem. Commun. 48 (2009) 7575.